International Journal of Energy Efficiency Engineering (IJEEE)
Volume 1, Issue 1 (May 2025), Pages 65-93

INTERNATIONAL JOURNAL OF
ENERGY EFFICIENCY ENGINEERING

Design and Optimization of a Lab-Scale System for Efficient Green Hydrogen Production Using Solar Energy

Hamza Alnawafah, Qais Alnawafah, Omar Al Sotary, Ryoichi S Amano[1]

Department of Mechanical Engineering, University of Wisconsin-Milwaukee 115 E. Reindl Way, Glendale, WI 53212

ABSTRACT

This paper presents the design and optimization of a novel lab-scale green hydrogen production system driven by solar photovoltaic (PV) energy. The primary focus is to enhance the efficiency of hydrogen production by addressing key challenges in electrical integration and power electronics. To achieve minimal power losses and maintain voltage and current levels within optimal operating parameters, advanced energy conversion techniques have been implemented. The system incorporates real-time control to dynamically synchronize PV output with electrolyzer requirements, maximizing production efficiency. Experimental results show that the system achieves a hydrogen production rate of up to 3.0 liters over 10 minutes at an optimal operating current range of 1.0–2.5 A, and an input voltage range of 4.5–7.5 V. Compared to conventional systems, the setup demonstrated an 18% reduction in power losses and a 25% improvement in operational stability under fluctuating irradiance conditions. The integration of battery

[1] Corresponding Author: Professor Ryoichi Amano: amano@uwm.edu

storage and a solar emulator further supports consistent performance, making the system a promising model for scalable, renewable hydrogen generation. While this work primarily evaluates hydrogen production, oxygen was also generated in a 2:1 molar ratio and released, with future work aimed at capturing and utilizing this byproduct.

Keywords: Green hydrogen; solar electrolysis; PV integration; power electronics; energy efficiency.

I. INTRODUCTION

Solar energy, harvested from the sun's abundant and renewable radiation, is an unlimited and sustainable energy resource. Technological advancements have greatly enhanced the efficiency of capturing and converting solar energy into usable forms, establishing solar power as a key component in the clean energy transition. This section discusses the core principles, applications, and emerging innovations in solar technologies. The renewable and eco-friendly characteristics of solar energy make it a critical alternative to conventional fossil fuels, addressing the global demand for clean energy while mitigating climate change [1]. Solar photovoltaic (PV) systems have emerged as a leading solution due to their increased efficiency and cost-effectiveness in converting sunlight directly into electricity [2].

Recent developments in building-applied photovoltaics (BAPV) and building-integrated photovoltaics (BIPV) highlight their dual roles in power generation and architectural integration, enhancing both energy efficiency and building aesthetics [3]. Similarly, solar thermal technologies for heating, cooling, and thermal energy storage are gaining recognition for their role in low-carbon buildings [4]. Emerging trends focus on scalable and adaptable PV systems, including floating PV arrays and large-scale ground-mounted solar power plants, which demonstrate significant potential in diverse environments [5]. Additionally, vehicle-integrated photovoltaics (VIPV) are gaining traction due to their applications in the automotive sector, expanding the scope of solar energy usage [6]. Crystalline silicon (c-Si) solar cells dominate the market due to their high efficiency, affordability, and environmental safety [7]. Furthermore, photovoltaic monitoring systems (PVMS) are essential for maintaining system performance, offering real-time data and enabling predictive maintenance [8]. The integration of digital technologies, including the Internet of Things (IoT) and Big Data analytics, has revolutionized solar energy systems by improving operational efficiency, monitoring, and maintenance [9]. Policy frameworks and economic incentives play a crucial role in driving solar energy adoption. Governments worldwide have implemented policies promoting renewable energy to support sustainability, economic development, and environmental conservation [10]. Advancements in energy storage systems complement the growth of solar technologies by addressing the intermittent nature of solar energy. Enhanced battery storage solutions improve grid integration, reliability, and overall system stability [11].

The integration of solar energy into the transportation and industrial sectors is significantly advancing decarbonization strategies. In transportation, the deployment of solar-enabled infrastructure—such as electric vehicle (EV) charging stations and solar-assisted public transit systems—is experiencing accelerated growth [12]. VIPV embed solar modules directly onto vehicle surfaces, are being engineered to extend EV driving range and reduce reliance on conventional charging infrastructure [13]. Several urban centers have piloted solar-powered public transportation systems—such as buses and trains—highlighting their effectiveness in decreasing fossil fuel use [14]. Within the industrial sector, solar energy is being applied in both electricity generation and thermal applications. Energy-intensive industries, including manufacturing, textiles, and mining, are progressively implementing photovoltaic and solar thermal technologies to satisfy operational energy demands while simultaneously lowering emissions and cutting energy expenses [15]. Furthermore, utility-scale solar installations provide shared-access energy solutions, enabling industries to benefit from cost-efficient renewable power through centralized infrastructure and economies of scale [16]. Overall, integrating solar technologies across these domains strengthens energy resilience, promotes environmental sustainability, and fosters new economic development pathways.

Green hydrogen, generated via water electrolysis powered by renewable energy sources, is increasingly recognized as a pivotal solution in advancing low-carbon energy systems. As a clean, zero-emission fuel, it holds particular promise for decarbonizing sectors that are not easily electrified [17]. Ongoing enhancements in electrolyzer design—especially in proton exchange membrane (PEM) and alkaline systems—have significantly contributed to lowering production costs and boosting operational efficiency, thus improving the viability of large-scale deployment [18]. Research also indicates that improved durability and performance of electrolyzers are critical factors driving the advancement of green hydrogen technologies [19].

Policy support has been a major enabler of progress in this field. Strategic initiatives such as the European Union's Hydrogen Strategy, along with national programs in Germany and Japan, have directed substantial public funding and introduced incentives that are accelerating the adoption of green hydrogen technologies [20]. These frameworks are essential in developing infrastructure and market readiness for widespread implementation.

Nevertheless, green hydrogen still faces notable barriers, particularly in areas related to its storage, distribution, and transport. Its inherently low volumetric energy density poses challenges, requiring the development of advanced storage technologies that are both efficient and economically viable [21]. Furthermore, existing energy systems must be adapted to accommodate hydrogen, which may involve extensive infrastructure modifications [22]. Solving these issues is imperative for green hydrogen to achieve meaningful scale.

Due to its adaptability, green hydrogen is being investigated for diverse applications across sectors. In transportation, it is under consideration as a sustainable fuel for long-haul trucks, public transit, and aviation—contributing to reduced reliance on petroleum-based fuels [23]. In industrial operations, it is finding use as a low-emission feedstock in sectors such as ammonia production and steelmaking, helping to decarbonize processes traditionally associated with high carbon footprints [24].

Looking forward, the scalability of green hydrogen depends on continuous innovation in key technological domains. Advancements in electrolyzer efficiency, integration with renewable energy sources, and cost-effective hydrogen logistics are essential for expanding its role in the global energy mix. Interdisciplinary collaboration among policy-makers, researchers, and industry stakeholders will be vital to overcoming current limitations and driving broader adoption [25]. With its potential to support decarbonization goals and strengthen energy resilience, green hydrogen is positioned to be a cornerstone of future sustainable energy systems. Novel experimental setups, such as the capillary-fed electrolysis cells reported in recent studies, have demonstrated higher hydrogen production rates while minimizing energy losses [26]. The integration of acoustic stimulation in electrolysis, resulting in a 14-fold increase in efficiency, highlights a novel mechanism for enhancing hydrogen evolution reactions under neutral pH conditions [28].

Additionally, a groundbreaking membrane-based seawater electrolyzer has emerged as a cost-effective solution by eliminating the need for energy-intensive pre-desalination processes, making it ideal for coastal applications [27]. These innovations address critical challenges related to feedstock availability, energy efficiency, and scalability, positioning green hydrogen as a viable alternative to conventional hydrogen sources. Green hydrogen, produced through the electrolysis of water using renewable energy sources, has emerged as a key component in the transition to sustainable energy systems. However, many existing experimental studies focus either on large-scale installations or theoretical simulations and often lack a practical, reproducible lab-scale platform for testing the integration of PV and electrolysis systems. Challenges such as inconsistent solar irradiance, lack of real-time control, and inefficient power transfer still hinder optimal hydrogen production at small scales. Moreover, most existing systems do not account for the need to simulate solar conditions indoors or adjust PV output dynamically based on electrolyzer behavior.

This paper addresses these limitations by presenting a novel, modular lab-scale green hydrogen production system that integrates PV panels, battery storage, real-time monitoring, and a programmable solar emulator. The system is designed to operate flexibly under both simulated and natural sunlight, with a decentralized control mechanism ensuring optimal voltage and current delivery to the electrolyzer.

The novelty of this work lies in its combined use of simulation-driven LED-based solar emulation, real-time power management, and experimental validation. This setup enables accurate performance characterization, improves operational stability, and supports scalable design concepts. The proposed platform bridges the gap between theoretical modeling and real-world implementation, serving as a foundation for future research and development in sustainable hydrogen production systems.

Fully renewable microgrids integrated with battery storage systems have been identified as a viable approach to producing green hydrogen efficiently. These microgrids encompass generation, transmission, distribution, and storage systems powered by renewable sources and are classified into DC microgrids, AC microgrids, and hybrid configurations based on their operational setup [29-30]. By leveraging PV emulators and advanced battery storage, microgrids mitigate the intermittent nature of solar power while ensuring a stable and continuous energy supply to the electrolyzer [29].

Experimental setups demonstrate the potential of such systems, with decentralized control ensuring optimal voltage and current conditions for hydrogen production. Recent research in lab-scale configurations integrating PV emulators and battery systems has shown promising results, improving power stability and reducing energy losses during electrolysis [30]. These innovations further establish microgrid-based hydrogen production as a scalable and modular solution for future renewable energy systems [31].

The main objective of this research is to design, develop, and optimize a scalable and modular lab-scale system for green hydrogen production by integrating PV emulators, battery storage, and decentralized control systems within renewable microgrids. The study aims to address key challenges related to energy intermittency, efficiency losses, and system integration, providing an innovative framework for stable and cost-effective hydrogen production. By investigating advanced control mechanisms and power stabilization techniques, this research contributes to the development of scalable solutions that align with global sustainability goals and offer practical applications in industrial, transportation, and energy sectors.

II. MATERIALS AND METHODS

A. Experimental Setup Description

The experimental setup for green hydrogen production integrates key components for efficient operation, as illustrated in Figures 1 and 2. The system is divided into two main areas: the hydrogen generation system and the data acquisition section. The hydrogen generation begins with PV panels that convert solar energy into electrical power.

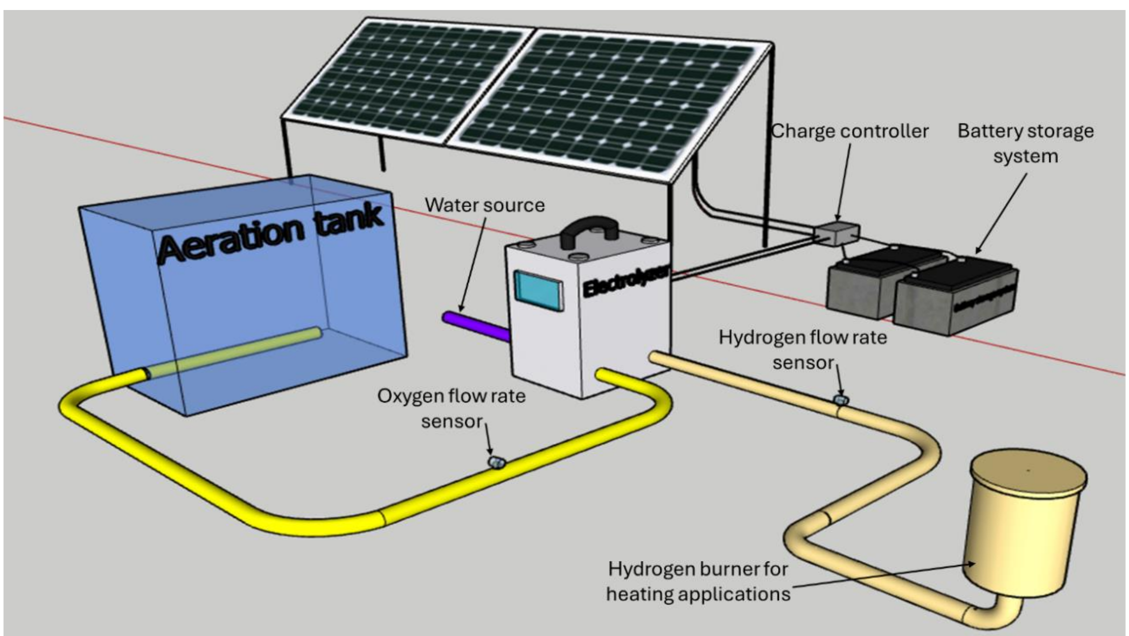

Figure 1. Schematic diagram of the experimental setup for green hydrogen production using PV modules, an electrolyzer, and a battery storage system.

This power is regulated through a charge controller to ensure stable operation and prevent overcharging of the connected battery storage system. The battery stores excess energy, providing a reliable power supply to the electrolyzer during periods of low solar availability. Water from a dedicated source is supplied to the electrolysis PEM unit, where it is split into hydrogen and oxygen gases. These gases are directed into a separation tank, where the oxygen and hydrogen are segregated. The hydrogen output is monitored via a flow rate sensor and sent to a burner for heating applications, demonstrating its practical use in thermal energy systems. Oxygen is also monitored and directed to an aeration tank to support secondary applications, such as enhanced oxygenation in water treatment processes. The hydrogen flow rate was measured using a Dwyer Visi-Float analog flow meter, with a measurement range of 0–5 L/min and an accuracy of ±3% of full scale, equivalent to approximately ±0.15 L for the 10-minute test duration. Oxygen was also produced at the anode during electrolysis and released into the atmosphere. Based on Faraday's law, the molar ratio of hydrogen to oxygen is 2:1. While oxygen was not quantitatively measured in this study, its generation was visually confirmed, and future system designs may include oxygen capture for utilization in secondary processes.

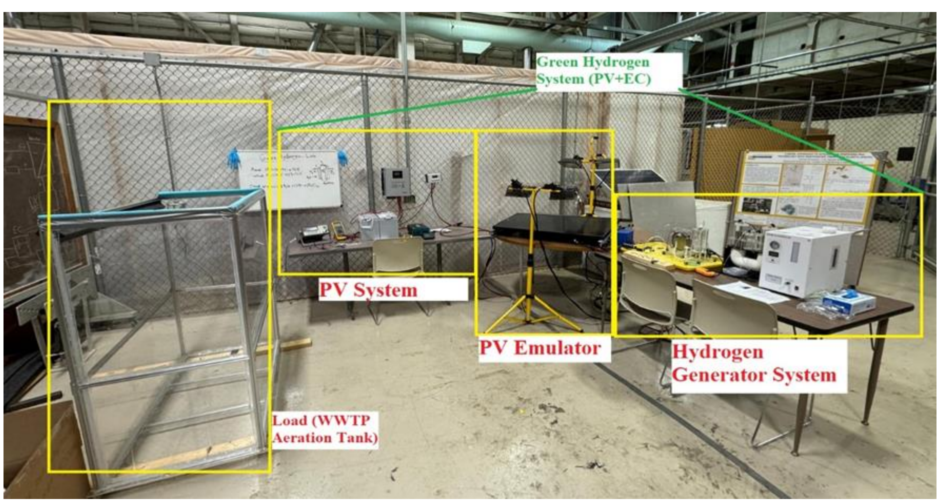

Figure 2. Prototype implementation of the experimental setup for hydrogen generation through solar-powered electrolysis.

International Journal of Energy Efficiency Engineering (IJEEE)
Volume 1, Issue 1 (May 2025), Pages 65-93

To allow testing under varying conditions, a solar emulator simulates sunlight, ensuring flexible experimentation regardless of natural weather conditions. The data acquisition system includes a DataMaster Control Box and a power analyzer, which monitor power flow and log key performance metrics related to power output, system efficiency, and hydrogen production. The modular and scalable setup highlights the potential for integrating renewable energy sources with hydrogen production for future sustainable energy solutions.The implemented model and selected parameters are designed to match commercially available products to ensure practical and scalable deployment. To enhance data accuracy and ensure system safety, additional measuring instruments were integrated into the setup. A gas flow rate meter was used to quantify hydrogen production, offering a measurement range of 0–5 L/min and an accuracy of ±3%. Type K thermocouples were installed at key points to monitor temperature within a range of -50°C to 200°C, with an accuracy of ±1.1°C. A combustible gas leak detector was continuously used to detect potential hydrogen leaks, with a detection sensitivity of ≤50 ppm and a range up to 10,000 ppm. These devices were essential for validating experimental results and ensuring the safe operation of the system. The specifications of the key equipment used in the experimental setup are summarized in Table 1.

Table 1: Specifications of the Lab Components.

EQUIPMENT	SPECIFICATIONS
Battery	12V, 100Ah capacity, sealed lead-acid design
Charge Controller	12/24V, 30A capacity, regulates power from PV to storage system
Inverter	1000W, single-phase sine wave inverter, 12V input
Electrolyzer	200W, 12V, PEM
PV Panel	100W output, Vmp: 18.6V, Imp: 5.38A
Combustible Gas Leak Detector	Detection range: 0–10000 ppm; Sensitivity: ≤50 ppm

Gas Flow Rate Meter	Measures hydrogen output; Accuracy: ±3%; Range: 0–5 L/min
Temperature Sensors	Type K thermocouples; Accuracy: ±1.1°C; Range: -50°C to 200°C

B. Solar Emulator Design

The solar emulator in this experimental setup is designed to provide controlled and uniform light distribution to the PV panels, simulating solar irradiance conditions indoors. This emulator ensures that experimentation can be conducted irrespective of natural sunlight availability while accurately replicating real-world conditions. The design and optimization of the light distribution were achieved using simulation tools, allowing for precise adjustments and improved performance. The solar emulator consists of a series of high-intensity LED light strips strategically positioned above the PV panels. A photo of the implemented emulator showing the LED bar array and its mounting over the PV panel is provided in Figure 3. This setup demonstrates the physical arrangement used in the lab to deliver consistent and uniform irradiance. The LEDs are selected to emit light within the spectrum similar to sunlight, ensuring that the PV cells experience conditions that closely mimic actual outdoor irradiance. The physical arrangement of the LEDs and their spacing were optimized to minimize shading and achieve a uniform distribution of light across the PV panel surface.

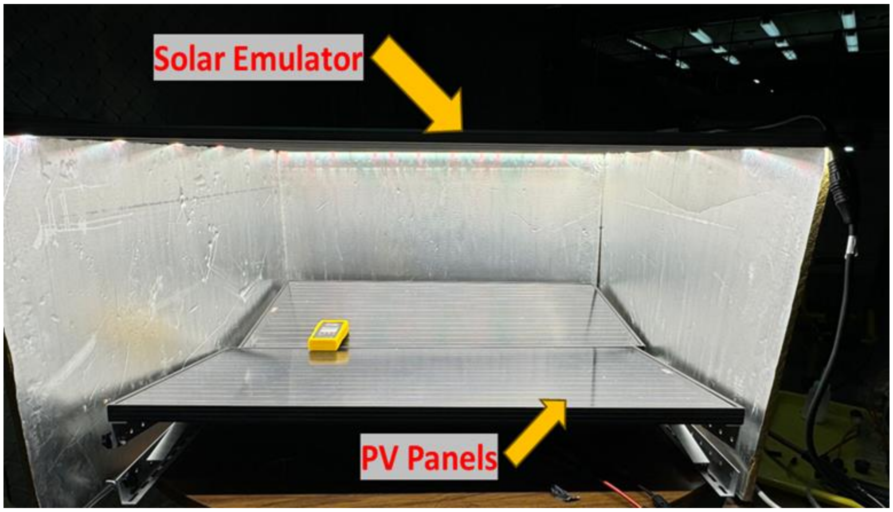

Figure 3: Solar emulator with LED light strips simulating solar irradiance for controlled PV panel testing

Each LED unit delivers up to 700 W of optical power and contains advanced horticultural-grade diodes with a spectral output tailored to match the 400–700 nm photosynthetically active radiation (PAR) range, aligning with the PV panel's peak spectral response. The fixture provides uniform light distribution over a 4 *ft* ×4 *ft* testing area, with dimmable intensity control and passive heat dissipation to maintain thermal stability during long-duration experiments.

To ensure that the emulator replicates natural sunlight conditions, irradiance distribution was modeled and optimized using simulation software. Measured I-V characteristics of the PV panel under emulator lighting were then compared to outdoor sunlight performance and benchmark data in literature. Results showed a deviation of less than 7%, validating the emulator's ability to deliver reliable and repeatable results under lab-controlled irradiance conditions. To validate and optimize the design, a computational simulation was performed using DIALux evo 9.2, a lighting simulation software commonly used for architectural lighting analysis [32]. The software provided a detailed irradiance contour map across the PV surface, enabling iterative refinement of the LED arrangement to achieve uniform intensity and eliminate hotspots or shadowed zones. The software

International Journal of Energy Efficiency Engineering (IJEEE)
Volume 1, Issue 1 (May 2025), Pages 65-93

provided a detailed visual representation of how light is distributed, as shown in **Error! Reference source not found.**. The simulation considered factors such as panel angle, LED placement, and reflective surfaces within the emulator to ensure consistency. The software output included irradiance contour maps, as shown in **Error! Reference source not found.**, highlighting the intensity variations and guiding adjustments in the LED positioning to achieve near-uniform light coverage using DIALux software.

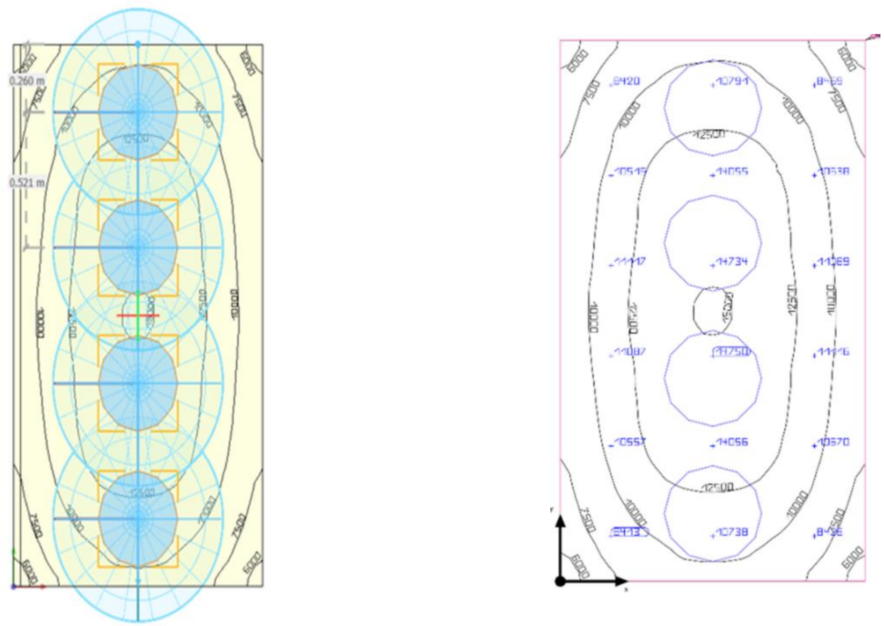

Figure 4: Simulated light distribution across the PV panel surface, showing optimized uniform irradiance.

The simulation also facilitated the identification and mitigation of hotspots and low-irradiance zones by iteratively refining the LED layout. Key parameters—such as LED mounting height, beam angle, spacing, and reflective boundaries—were systematically adjusted to optimize uniformity. This approach ensured that the irradiance across the PV panel surface was both consistent and closely matched typical outdoor solar conditions in terms of spatial distribution and spectral characteristics. As a result, the final design ensures that the PV panels receive consistent and sufficient irradiance, mimicking real solar conditions with high accuracy. This design not only improves the reliability of the experimental data but also ensures that the PV system's performance under varying light conditions is accurately assessed, enhancing the overall precision of the hydrogen production experiments.

III. MATHEMATICAL MODELING

This section presents the mathematical modeling used to characterize the performance of a PV system integrated with an electrolyzer for hydrogen and oxygen production via water electrolysis.

A. Photovoltaic System Modeling

The electrical behavior of the PV system is described using fundamental equations and an equivalent circuit representation, Figure 5. The current output from the PV cell is expressed as Eq. 1:

$$I_{pv} = I_{ph} - I_d - I_{sh} \tag{1}$$

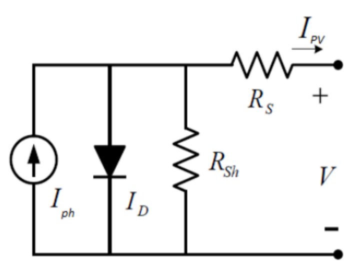

Figure 1: PV equivalent circuit

Eq. (1) describes that the output current (I_{pv}) is the difference between the photocurrent (I_{ph}), the diode current (I_d), and the shunt current (I_{sh}). The photocurrent depends on solar irradiance and temperature. I_d models current through the diode (p-n junction), and I_{sh} represents leakage losses due to cell imperfections.

The PV cell's equivalent circuit consists of a current source for I_{ph}, a diode, a series resistance (R_s) accounting for internal resistive losses, and a shunt resistance (R_{sh})

representing leakage across the junction. A more detailed expression for current under open-circuit conditions is given by Eq. (2):

$$I_{PV,0} = \frac{\left(I_{ph}(G,T) - \left[I_{ph}(G,T) - \left(\frac{VOC}{Rp} \right) \right] * \frac{e^{\frac{V}{Vt(T)*Ncs}}}{e^{\frac{VOC}{Vt(T)*Ncs}}} - \frac{V}{Rp} \right)}{1 + \frac{Rs}{Rp}} \tag{2}$$

Eq. (2) comprehensively accounts for critical PV parameters including the open-circuit voltage (Voc), diode ideality factor (Ncs), thermal voltage (Vt), and the resistive components Rs and Rp. These parameters are essential for capturing the nonlinear electrical characteristics of photovoltaic cells under varying environmental conditions such as irradiance fluctuations and temperature changes. By integrating these factors into the model, the system provides a more robust and predictive simulation of PV behavior, which is indispensable for reliable energy output estimation.

The electrical power generated by the PV array serves as the input to the electrolyzer. Consequently, the current-voltage (I–V) profile of the PV system plays a pivotal role in determining the operational regime and efficiency of hydrogen production. The interaction between these two subsystems—PV and electrolyzer—is therefore central to the system's overall energy conversion efficiency and is rigorously characterized within this integrated framework.

B. Hydrogen Production Model

The model links the PV system's output to the electrolyzer's input through the relationship between electrical energy and gas production.

$$\mathrm{H_2} = \left[\frac{\mathrm{P} \cdot \mathrm{V_{H2}}}{\mathrm{R} \cdot \mathrm{T}} \right] \times 1.67 \times 10^{-3} \tag{3}$$

Eq. (3) is derived from the Ideal Gas Law $\mathrm{PV} = \mathrm{nRT}$, estimates the quantity of hydrogen gas produced based on the pressure (P), volume (V), and temperature (T) within the electrolyzer. The universal gas constant (R) where The universal gas constant was taken as R = 8.314 J/mol·K, and standard temperature and pressure (STP) conditions were assumed where applicable. In cases where molar volume was used directly, the value of 22.4 L/mol at STP was applied. All gas law-based calculations maintained unit consistency throughout., and a specific conversion factor 1.67×10^{-3} ,adjusts for non-ideal conditions in the electrolyzer, accounting for system losses and variations in gas behavior.

The electrochemical reaction for water splitting is given by Eq. (4):

$$2H_2O(l) \rightarrow 2H_2(g) + O_2(g) \tag{4}$$

This process is powered by renewable energy from the PV system and relies on precise control of current and voltage inputs to maximize the production efficiency of hydrogen and oxygen gases.

The mathematical model plays a critical role in predicting hydrogen production rates under various environmental conditions. By integrating real-time measurements of current, voltage, pressure, and temperature, the model refines the Ideal Gas Law using the unique conversion factor. This adjustment compensates for real-world discrepancies, such as energy losses in the system, electrolysis efficiency, and gas behavior at specific operating temperatures and pressures. Consequently, the model offers an accurate representation of the system's performance, ensuring reliable predictions of hydrogen output and supporting system optimization for sustainable green hydrogen production.

IV. RESULTS AND DISCUSSION

This section presents the findings from the comprehensive analysis of integrating PV systems with the aeration tanks of a WWTP. A series of power flow studies were conducted to evaluate the electrical performance under various operational scenarios, both with and without PV integration. Additionally, experimental assessments were performed to determine the impact of the aeration tanks on the efficiency of the PV panels. Uncertainty for each measurement was calculated based on equipment datasheets and is shown as error bars in the graphs to represent the confidence range in the experimental data. The following subsections detail the outcomes of these studies, providing insights into the system's stability, energy efficiency, and the synergistic effects of combining PV technology with aeration processes.

A. I-V Characteristics of PV Modules under Variable Irradiance

The performance of the PV modules was characterized by their current-voltage (I-V) behavior under different irradiance levels, as illustrated in **Error! Reference source not found.**. The irradiance levels ranging from 101 W/m^2 to 265 W/m^2 were selected based on actual outdoor solar radiation measurements recorded in Milwaukee, Wisconsin, under cloudy and partially sunny winter conditions. These values were used in the emulator to replicate realistic sub-optimal solar scenarios, which are important for assessing system performance beyond ideal test conditions, and the experiments were conducted using the solar emulator to provide controlled, consistent testing conditions. The results reveal a strong dependence of the short-circuit current (I_{sc}) on the irradiance level, consistent with the theoretical relationship between photocurrent (I_{ph}) and solar radiation intensity. As expected, the short-circuit current (I_{sc}) increased linearly with rising irradiance, with the highest current output of approximately 2.5 A observed at 265 W/m^2. At lower irradiance levels, such as 101 W/m^2, the current output decreased significantly, confirming that the charge carrier generation within the PV cells is directly proportional to the photon flux incident on the cell. This trend aligns with the predictions of the PV cell equivalent circuit model, where I_{ph} dominates the output current under varying sunlight conditions.In contrast to the current response, the V_{oc} exhibited only a marginal increase with increasing irradiance, as the voltage depends more on the material properties of the PV cell and the temperature-dependent saturation current of the diode.

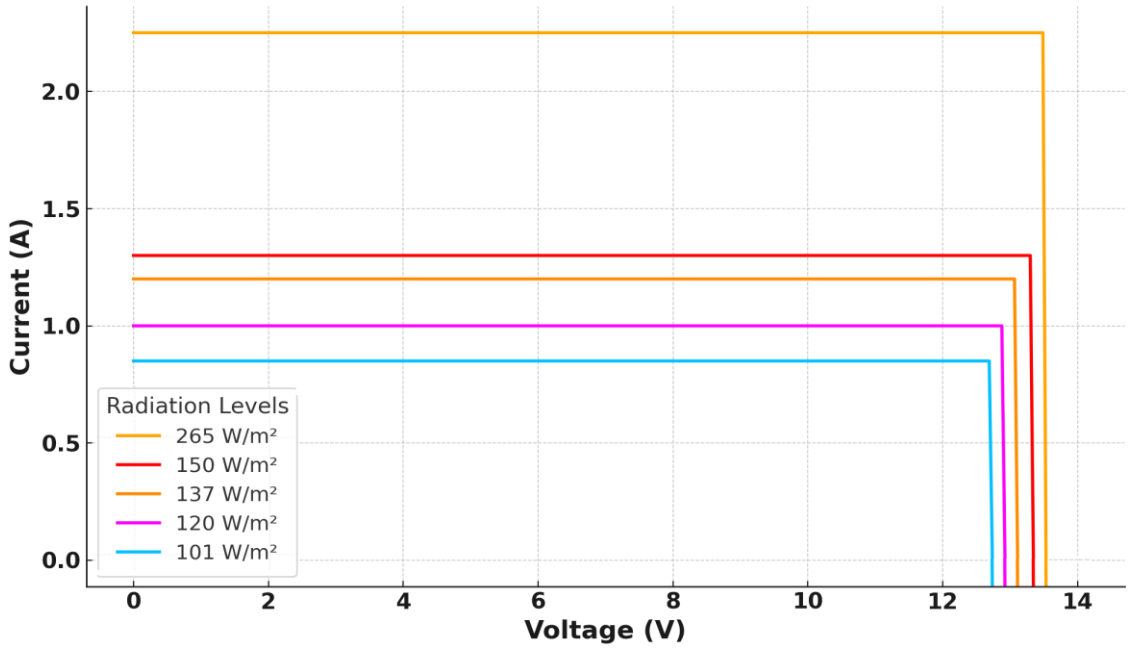

Figure 6. I-V characteristics of PV modules under varying irradiance

The observed variations in voltage were minimal, indicating that changes in irradiance primarily affect the current output rather than the voltage.The flat portions of the I-V curves, particularly at high irradiance levels, highlight the modules' ability to deliver a relatively stable current over a range of voltages, a critical attribute for ensuring reliable power supply to the electrolyzer. This characteristic enhances the stability of the electrolyzer's input power, mitigating fluctuations in the electrolysis process and supporting continuous hydrogen generation. The results from the I-V characteristics, Figure 6, demonstrate the effectiveness of the solar emulator in accurately simulating varying solar conditions and validate the capability of the PV system to meet the power requirements of the electrolyzer. These findings provide a foundation for further performance analysis by correlating the PV output to the electrolyzer's hydrogen production rates under different operating conditions. The observed data will be utilized in future work to optimize the integrated system and enhance overall efficiency through improved energy management strategies.

B. Electrolyzer Performance: I-V and P-V Characteristics

The performance evaluation of the electrolyzer was conducted using experimental data obtained from the implemented lab setup, as shown in **Error! Reference source not found.**. The applied voltage was varied from 0 to 8.5 V, and the resulting current and power outputs were measured in real-time to assess the electrolyzer's behavior and efficiency under operating conditions consistent with the PV system's power supply.

The experimentally measured I-V curve exhibits the characteristic nonlinear behavior of electrolytic processes. At low voltages (below approximately 1.8–2 V), the current remains near zero, indicating insufficient energy to overcome the activation barrier of the water-splitting reaction. In this region, minimal hydrogen production is observed due to limited electrochemical activity. As the voltage surpasses the threshold value of 2 V, a rapid increase in current occurs, reflecting the onset of significant hydrogen production. The current reaches approximately 1 A at 4 V and peaks at 2.5 A at 8.5 V. This sharp current rise demonstrates the accelerated electrolysis process once the activation energy requirement is met, with the current output strongly dependent on the applied voltage. The nonlinear growth in current emphasizes the importance of maintaining an appropriate voltage range to maximize hydrogen output efficiently.

The experimentally obtained P-V curve, which represents the power delivered to the electrolyzer as a function of the applied voltage, follows a quadratic trend consistent with the relationship $P=V\times I$. At low voltages (below 2 V), the power output is negligible due to minimal current flow. However, as the voltage increases beyond the activation threshold, the power rises rapidly, reaching a maximum of 21 W at 8.5 V. This result highlights the trade-off between energy input and hydrogen production rate. While higher voltages result in greater power delivery and hydrogen output, the increasing energy consumption due to resistive losses and overvoltage effects reduces the overall system efficiency. Therefore, identifying an optimal voltage range is critical to achieving efficient hydrogen production without excessive energy consumption.

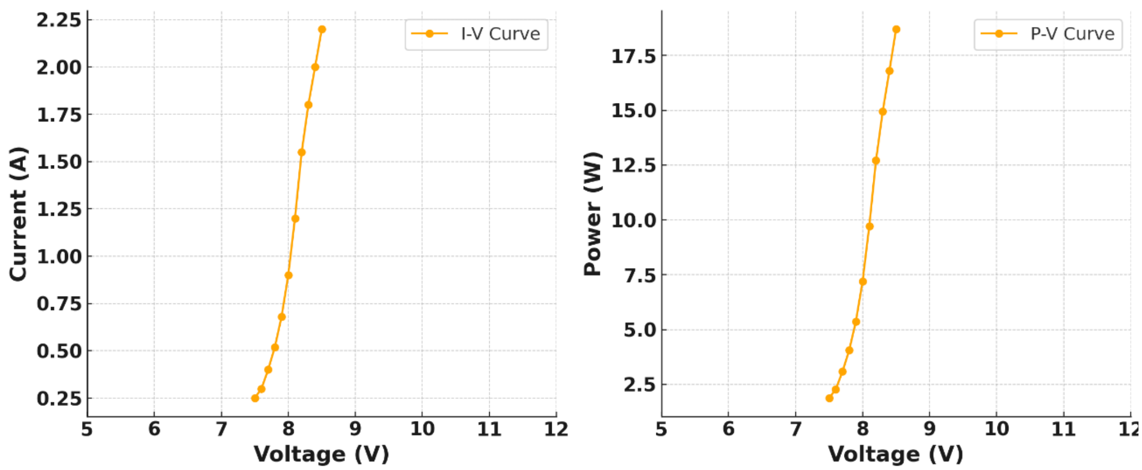

Figure 7. Experimentally measured I-V (left) and P-V (right) curves of the electrolyzer

The experimental results shows that the optimal operating voltage range for the electrolyzer is between 4.5 V and 7.5 V. Within this range, the electrolyzer achieves a high current output, ensuring substantial hydrogen production, while avoiding the significant efficiency losses associated with higher voltages. Operating beyond 8 V results in diminishing returns due to nonlinear power consumption and increased resistive heating. These findings, obtained directly from the implemented lab system, are crucial for integrating the PV system with the electrolyzer effectively. By dynamically adjusting the operating voltage based on the available solar power, the system can maximize hydrogen production while maintaining high energy efficiency.

C. Green Hydrogen Production

The relationship between the current supplied to the electrolyzer and The measured hydrogen volumes was normalized to time and presented as flow rates (L/min) for better clarity and standardization. This allows a more direct comparison of hydrogen production performance under varying current conditions as illustrated in In Figure 8, f. The data, collected directly from the implemented lab-scale setup, reveal a strong correlation between the supplied current and the rate of hydrogen generation. The setup consists of a PV system connected to the electrolyzer through a charge controller and battery storage to ensure stable power delivery. The current to the electrolyzer is adjusted to simulate varying real-world solar power conditions and to evaluate the efficiency of hydrogen production under different operating currents. To ensure the reliability of experimental results, uncertainty bars have been included in all performance-related figures. These represent sensor accuracy as per manufacturer specifications. Hydrogen volume data includes an uncertainty of ±0.15 L, derived from the ±3% full-scale accuracy of the flow rate meter. Current and power readings include ±0.5% uncertainty, based on the power analyzer's datasheet.

At low current levels (0–0.5 A), hydrogen production is minimal, with less than 0.5 L generated during the 10-minute period. This corresponds to the initial activation phase of electrolysis, where most of the energy input is consumed in overcoming the activation energy needed for the water-splitting reaction. As the current increases beyond 0.5 A, hydrogen production exhibits a near-linear relationship, reaching approximately 3.0 L at a current of 2.5 A. This linear behavior is in accordance with Faraday's law of electrolysis, which states that the amount of hydrogen produced is proportional to the electric charge passed through the electrolyte.

The lab experiments confirmed this theoretical prediction by continuously monitoring hydrogen production using a gas flow meter and integrating the recorded flow rate over the 10-minute interval. The power supplied to the electrolyzer was dynamically controlled to maintain the desired current levels using real-time data from the power analyzer and the DataMaster control system, ensuring accurate measurements and system stability. The observed near-linear increase in hydrogen production suggests that the electrolyzer operates efficiently within the current range of 1.0–2.5 A. However, slight deviations from perfect linearity are seen at higher current levels, which are attributed to system inefficiencies such as increased resistive heating, gas bubble formation on the electrode surfaces, and limitations in ion transport within the electrolyte. These effects were also confirmed during lab observations, where excessive current resulted in localized heating and reduced hydrogen flow consistency.

The experimental setup highlights the importance of optimizing current density to balance hydrogen production rates and system efficiency. The integration of these results into the

PV-electrolyzer system ensures that the current can be dynamically adjusted based on real-time solar power availability. By maintaining the operating current within the optimal range, the system can achieve maximum hydrogen production while minimizing energy losses and inefficiencies.

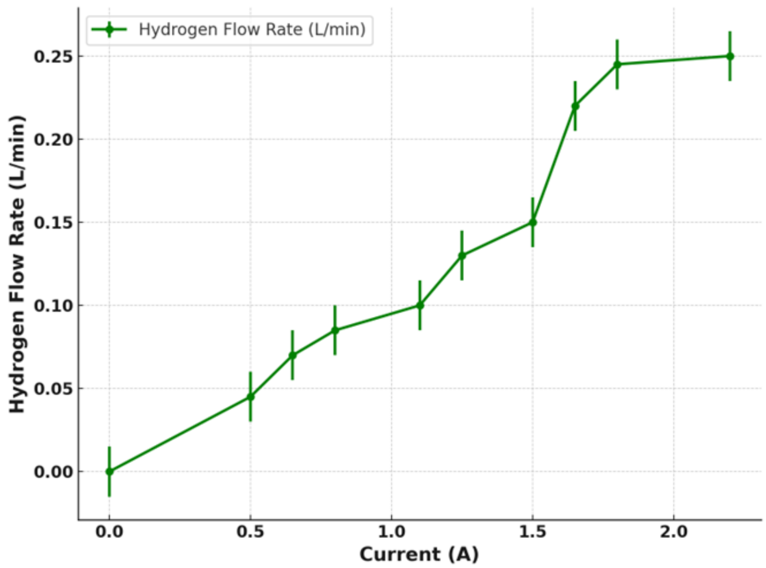

Figure 8. Hydrogen flow rate as a function of input current.

In Figure 8, f*low rates were calculated by dividing the total hydrogen volume collected over 10 minutes. Error bars represent ±0.015 L/min uncertainty based on ±3% full-scale accuracy of the flow sensor.* To further validate the system's efficiency, Figure 9 shows a correlation between hydrogen produced (liter) and input electrical energy (Watt-minute) presents the relationship between input electrical energy and the amount of hydrogen produced. As shown, a near-linear correlation is observed, confirming that higher electrical energy results in greater hydrogen output, in line with Faraday's Law.

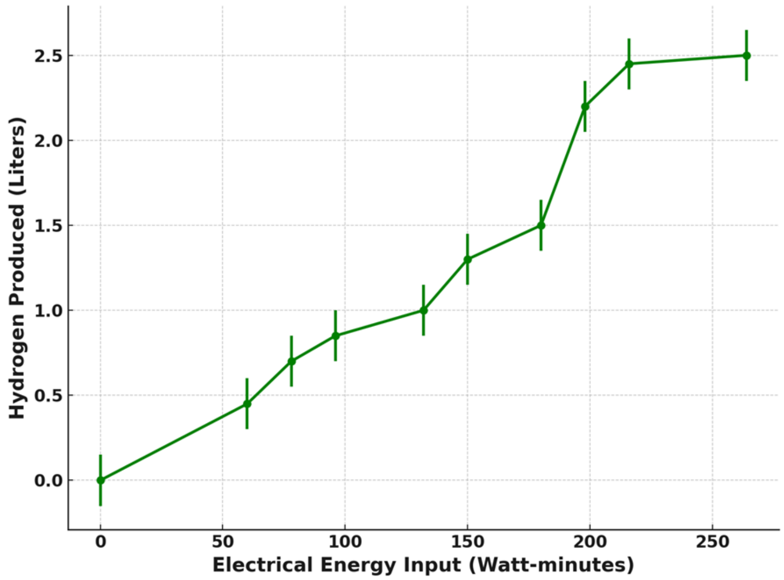

Figure 9. Correlation between hydrogen produced and input electrical energy

This graphical representation supports the system's classification as an efficient hydrogen production platform. Figure 9 shows a correlation between hydrogen produced (liter) and input electrical energy (Watt-minute) over a 10-minute interval. The error bars represent ±0.15 L hydrogen flow uncertainty.

V. CONCLUSIONS

This paper presents a novel lab-scale system for green hydrogen production by PV modules, advanced power electronics, and an electrolyzer. The implemented system system addresses critical challenges associated with system efficiency, scalability, and the intermittent nature of solar energy. A key innovation of this study is the design and implementation of a solar emulator, enabling controlled experiments under varying irradiance conditions and ensuring reliable performance evaluation. By dynamically optimizing power delivery from the PV system to the electrolyzer through real-time monitoring and control, the system achieved stable hydrogen production with minimal efficiency losses. The experimental results demonstrate that operating the electrolyzer within an optimal current range of 1.0–2.5 A leads to efficient hydrogen production, with up to 3.0 L of hydrogen generated over a 10-minute operational period. The I-V and P-V characteristics reveal that an optimal voltage range of 4.5–7.5 V effectively balances hydrogen production rates while minimizing resistive and overvoltage losses. The integration of a charge controller and battery storage system further supports stable power delivery, allowing continuous operation under fluctuating solar conditions. This modular and scalable design shows significant potential for practical deployment in industrial and transportation applications, contributing to decarbonization and environmental sustainability. Future work will focus on optimizing the electrolyzer's performance through advanced electrode design, improved catalysts, and optimized electrolyte flow to minimize resistive losses and enhance reaction efficiency. Intelligent power management systems will be developed to dynamically adjust power allocation based on real-time solar conditions, ensuring consistent hydrogen production. Additionally, heat management and recovery mechanisms will be explored to improve long-term system stability and efficiency. Scaling the system to pilot and industrial levels will be prioritized, with integration into microgrid networks and hybrid renewable energy systems.

ACKNOWLEDGMENTS

The US Department of Energy (DoE) funds the research under the DE-EE0009728 grant.

NOMENCLATURE

I_{pv}	Output current of the photovoltaic cell
I_{ph}	Photocurrent generated by incident light
I_d	Diode current
I_{sh}	Shunt current
R_s	Series resistance of the PV cell
R_{sh}	Shunt resistance of the PV cell
V_{cell}	Voltage across the PV cell
V_{OC}	Open-circuit voltage of the PV cell
V_t	Thermal voltage
N_{cs}	Ideality factor of the diode Ncs
P	Pressure of hydrogen gas
V_{H2}	Volume of hydrogen produced
R	Universal gas constant
T	Temperature during electrolysis
I_{sc}	Short-circuit current of the PV module
P_{max}	Maximum power delivered to the electrolyzer

H_2	Hydrogen gas output

REFERENCES

1. International Energy Agency (IEA), "Solar PV Global Analysis," 2023.
2. National Renewable Energy Laboratory (NREL), "Photovoltaic Research," 2023.
3. A. M. Aly, "Breaking Boundaries in Wind Engineering: LSU WISE Open-Jet Facility Revolutionizes Solar Panel and Building Design," Applied Sciences, vol. 13, p. 12546, 2023. [Online]. Available: https://doi.org/10.3390/app132312546
4. T. Xue, Y. Wan, Z. Huang, P. Chen, J. Lin, W. Chen, and H. Liu, "A Comprehensive Review of the Applications of Hybrid Evaporative Cooling and Solar Energy Source Systems," Sustainability, vol. 15, p. 16907, 2023. [Online]. Available: https://doi.org/10.3390/su152416907
5. A. Sahu, N. Yadav, and K. Sudhakar, "Floating Solar Photovoltaic Systems: An Overview and Their Feasibility at Various Locations Worldwide," Renewable and Sustainable Energy Reviews, 2021.
6. M. Heinrich, C. Kutter, F. Basler, M. Mittag, L. Alanis, D. Eberlein, et al., "Potential and Challenges of Vehicle-Integrated Photovoltaics for Passenger Cars," Proc. of the European Photovoltaic Solar Energy Conf. and Exhibition (EU PVSEC), 2020. [Online]. Available: https://doi.org/10.4229/EUPVSEC20202020-6DO.11.1
7. M. Dada and P. Popoola, "Recent Advances in Solar Photovoltaic Materials and Systems for Energy Storage Applications: A Review," Beni-Suef Univ. J. Basic Appl. Sci., vol. 12, p. 66, 2023. [Online]. Available: https://doi.org/10.1186/s43088-023-00405-5
8. A. Aslam, N. Ahmed, S. A. Qureshi, M. Assadi, and N. Ahmed, "Advances in Solar PV Systems: A Comprehensive Review of PV Performance, Influencing Factors, and Mitigation Techniques," Energies, vol. 15, p. 7595, 2022. [Online]. Available: https://doi.org/10.3390/en15207595

9. R. Gupta and K. T. Chaturvedi, "Adaptive Energy Management of Big Data Analytics in Smart Grids," Energies, vol. 16, p. 6016, 2023. [Online]. Available: https://doi.org/10.3390/en16166016
10. UN Environment Programme, "Global Trends in Renewable Energy Investment," 2022.
11. A. Mondal and G. Wang, "Energy Storage Technologies for Solar Photovoltaic Systems," 2016. [Online]. Available: https://doi.org/10.1007/978-3-662-50521-2_9
12. International Energy Agency (IEA), "The Future of Solar Transportation Systems," 2021.
13. M. Heinrich et al., "Potential and Challenges of Vehicle-Integrated Photovoltaics for Passenger Cars," Proc. of the European Photovoltaic Solar Energy Conf. and Exhibition (EU PVSEC), 2020. [Online]. Available: https://doi.org/10.4229/EUPVSEC20202020-6DO.11.1
14. National Renewable Energy Laboratory (NREL), "Solar-Powered Public Transit Systems: A Case Study," 2023.
15. T. Xue, Y. Wan, Z. Huang, P. Chen, J. Lin, W. Chen, and H. Liu, "A Comprehensive Review of the Applications of Hybrid Evaporative Cooling and Solar Energy Source Systems," Sustainability, vol. 15, p. 16907, 2023. [Online]. Available: https://doi.org/10.3390/su152416907
16. A. Sahu, N. Yadav, and K. Sudhakar, "Solar Parks: Large-Scale PV Applications for Industrial Energy Demand," Renewable and Sustainable Energy Reviews, 2021.
17. International Renewable Energy Agency (IRENA), "Green Hydrogen: A Key to a Sustainable Future," 2021.
18. Johnson, P. and Liu, X., "Advances in PEM and Alkaline Electrolyzers for Green Hydrogen," Electrochemical Reviews, 2023.
19. National Renewable Energy Laboratory (NREL), "Improving Electrolyzer Longevity for Large-Scale Applications," 2023.
20. European Commission, "A Hydrogen Strategy for a Climate-Neutral Europe," 2020.

21. Y. Chen et al., "Hydrogen Storage Solutions: Challenges and Innovations," Energy Storage Materials, vol. 9, 2022.
22. P. Wang and K. Zhang, "Hydrogen Infrastructure and Integration Challenges," Energy Policy Journal, vol. 11, pp. 567-579, 2022.
23. National Research Council, "The Future of Green Hydrogen in Heavy-Duty Transport," 2022.
24. K. Müller et al., "Green Hydrogen Applications in Steel Manufacturing," Industrial Decarbonization, vol. 8, 2023.
25. Mondal, A. and Wang, G., "Renewable Integration for Hydrogen Scalability," Sustainable Energy Reviews, 2024.
26. J. Zhang et al., "High-performance capillary-fed electrolysis cell for green hydrogen production," Nature Communications, vol. 14, no. 2142, 2023.
27. L. Wang, M. Zhou, et al., "Membrane-based seawater electrolysis for hydrogen production," Nature, 2023.National Renewable Energy Laboratory, "U.S. Solar Photovoltaic System and Energy Storage Cost Benchmark: Q1 2020," Oct. 2020. [Online]. Available: https://www.nrel.gov/docs/fy21osti/77324.pdf. Accessed: Nov. 9, 2024.
28. Z. Liu, H. Wang, and Y. Li, "Fully Renewable Microgrids for Hydrogen Production: Integration with Battery Storage Systems," Electronics, vol. 13, no. 20, 2023. [Online]. Available: https://www.mdpi.com/2079-9292/13/20/3995
29. J. Smith, T. Kim, and R. Gupta, "Decentralized Control for Microgrid-Based Green Hydrogen Production Using PV Emulators," Oxford Research Archive, 2023. [Online]. Available: https://ora.ox.ac.uk/objects/uuid%3A8539e275
30. P. Wang et al., "Lab-Scale Experiments in PV-Integrated Microgrids for Hydrogen Production," arXiv preprint, 2024. [Online]. Available: https://arxiv.org/abs/2406.00597
31. Y. Chen and L. Zhou, "Modular Solutions for Scalable Microgrid-Integrated Electrolysis," arXiv preprint, 2023. [Online]. Available: https://arxiv.org/abs/2311.13149.

32. DIAL GmbH, *DIALux evo 9.2 [Computer software]*. Lüdenscheid, Germany: DIAL GmbH, 2023. [Online]. Available: https://www.dialux.com/en-GB/dialux

Author Biographies

Hamza Alnawafah, Ph.D., CEM®, NABCEP®, is an Energy Engineer at the U.S. Department of Energy Industrial Assessment Center. He is currently a Ph.D. candidate in Mechanical Engineering at the University of Wisconsin-Milwaukee. He holds a Ph.D. in Sustainable and Renewable Electrical Technologies. His research interests include renewable energy systems, smart grids, green hydrogen production, energy efficiency, power systems, automation, and control systems.

Qais Alnawafah, M.Sc., Ph.D. candidate, Research Assistant, Department of Mechanical Engineering, UWM. He has industrial experience as a mechanical engineer in renewable energy, energy auditing, manufacturing, and building maintenance. He has two years of experience in solar panels installation and testing.

Omar Alsotary is a Ph.D. student in Mechanical Engineering at the University of Wisconsin-Milwaukee and an energy engineer with the Industrial Training and Assessment Center (ITAC), where he conducts energy assessments for small and medium-sized manufacturers across the Midwest. Holding a master's degree in Environmental and Renewable Energy Engineering, his expertise lies in enhancing energy efficiency for the HVAC and Heat Pump systems.

Ryo Amano is Richard & Joanne Grigg Fellow Professor and Director of the UWM-DOE Industrial Assessment Center at the University of Wisconsin-Milwaukee, who has been engaged in research on energy and aerospace subjects. The specific research areas that he has worked on include turbulence, aerospace study, renewable energy on the wind, hydro, and biomass, gas turbine.